Citation: Weizhong Zhang, Xiaoan Yan, Maoyou Ye, et al. An improved wind turbine bearing fault diagnosis method based on POSGMD and ICNN under strong noise scenarios. *Journal of Harbin Institute of Technology (New Series)*, 2025, 32(2): 00-00. DOI: 10.11916/j.issn.1005-9113.2024102.

An Improved Wind Turbine Bearing Fault Diagnosis Method Based on POSGMD and ICNN Under Strong Noise Scenarios

Weizhong Zhang, Xiaoan Yan, Maoyou Ye, Xing Hua and Dong Jiang*

(*School of Mechatronics Engineering, Nanjing Forestry University, Nanjing 210037, China*)

Abstract: Owing to the harsh conditions, wind turbine bearings are prone to faults, and the resulting fault information is easily submerged by strong noise disturbance, making conventional diagnosis challenging. Therefore, this study presents an innovative bearing fault diagnosis approach predicated on parameter-optimized symplectic geometry mode decomposition (POSGMD) and improved convolutional neural network (ICNN). Firstly, assisted by the relative entropy-based adaptive selection of embedding dimension, a POSGMD is presented to adaptively decompose the collected bearing vibration signals into various symplectic geometry components (SGC), which can solve the problem of manual selection of the embedding dimension in the raw symplectic geometry mode decomposition (SGMD). Meanwhile, the signal reconstruction on the decomposed SGC is conducted based on kurtosis-weighted principle to obtain the reconstructed signals. Subsequently, the continuous wavelet transform (CWT) of the reconstructed signals is calculated to generate the corresponding time-frequency images as sample set. Finally, an ICNN is introduced for model training and automatic recognition of bearing faults. Two case studies are used to validate the presented method's efficacy. Comparing the presented method with traditional fault diagnosis methods, experimental results show that it can achieve greater identification accuracy and superior anti-noise resilience. This work provides a practical and effective solution for fault diagnosis in wind turbine bearings, contributing to the timely detection of faults and the reliable operation of wind turbines or other rotational machinery in industrial applications.

Keywords: symplectic geometry mode decomposition; convolutional neural network; deep learning; rolling bearing; fault diagnosis; anti-noise robustness

CLC number: TM315, TH133 **Document code**: A **Article ID**: 1005-9113(2025)02-0000-19

0 Introduction

As an integral mechanical element within wind power generator, wind turbine bearings are extensively used to minimize frictional losses in wind power equipment. However, prolonged high-speed operation can lead to various degrees and types of damage in wind turbine bearings, resulting in wind power equipment malfunction and operational disruptions[1]. Moreover, wind turbine bearing faults not only inflict significant economic losses on factories but also pose a serious threat to wind farm enterprise staff safety. Consequently, the development of effective methods for diagnosing wind turbine bearing failures is a key safeguard for the safe and dependable operation of wind power facilities and the prevention of injuries to personnel on site[2].

The operating conditions of wind power equipment are typically complex. When wind turbine bearing faults occur, the collected signals often show non-linear and non-stationary features, including the useful components and various noise interference[3-4]. In existing research, many scholars have used adaptive signal decomposition techniques to analyze the acquired vibration signals from the bearings, the objective is to eliminate superfluous components while extracting pertinent fault feature information[5]. Empirical Mode Decomposition (EMD) is a prominent signal decomposition algorithm. However,

Received 2024-11-15.

Sponsored by the Jiangsu Association for Science and Technology Youth Talent Support Project (Grant No. JSTJ-2024-031), the National Natural Science Foundation of China (Grant No. 52005265), and the Natural Science Fund for Colleges and Universities in Jiangsu Province (Grant No. 20KJB460002).

* Corresponding author. Xiaoan Yan, Ph.D, Associtate professor. Email: yanxiaoan89@sina.com.

during the decomposition process, EMD is prone to endpoint effects and mode mixing issues[6]. To address these challenges, the ensemble empirical mode decomposition (EEMD) and its enhanced edition (i.e., complementary ensemble empirical mode decomposition (CEEMD)) are presented for suppressing the mode mixing phenomena through the introduction of white noises into the original signal. The EEMD method facilitates better decomposition of non-stationary signals, which can enhance the accuracy and reliability of signal decomposition. However, the introduction of variables during the addition of white noise lacks adaptability[7-8]. Intrinsic time-scale decomposition (ITD) has good adaptability by utilizing a linear transformation approach to extract baseline signals. Nevertheless, during the decomposition process of ITD, the obtained components are susceptible to the spiky phenomenon, leading to distortions in instantaneous amplitude and frequency[9]. Empirical wavelet transform (EWT) stands out as a multi-resolution signal analysis approach that can decompose the input signal into several sub-band signals and provide a signal reconstruction. However, EWT is prone to segmenting many invalid components and has the disadvantages of long computation time and mode aliasing phenomenon. The variational mode decomposition (VMD) represents a contemporary approach to signal decomposition, which has witnessed significant utilization within the realm of bearing fault diagnosis. Unfortunately, despite VMD has strong separation capabilities for non-stationary signals, two key parameters (i.e., number of modes and penalty factor) affect its decomposition performance. Besides, adjustments to these parameters often require empirical or trial-and-error methods[10-11].

SGMD is an inventive adaptive signal analysis approach compared with the traditional decomposition method (i.e., EMD, ITD and EEMD). SGMD offers advantages such as preserving the inherent characteristics of the original time series, suppressing mode mixing, and demonstrating robustness against noise. As such, it has found numerous successful applications within the realm of bearing fault diagnosis[12-13]. Wang et al.[14] presented an inventive approach for gear fault diagnosis utilizing SGMD and Autogram. The superiority of this method was validated through simulation and gear fault data. Guo et al.[15] introduced an adjustable SGMD approach for weak feature extraction and composite fault detection using periodic kurtosis entropy. Its effectiveness in fault diagnosis was corroborated through numerical simulations and experimental verification. Liu et al.[16] presented a novel approach for rolling bearing fault diagnosis, utilizing partially reconstructed symplectic geometry mode decomposition (PRSGMD), enhancing the robustness and efficacy of bearing fault diagnosis. Yan et al.[17] presented a smart fault diagnosis approach predicated upon SGMD, improved multiscale symbolic dynamic entropy (IMSDE), and multiclass relevance vector machine (MRVM). Empirical findings showcased the elevated precision in identification afforded by this approach. However, in the aforementioned studies, the embedding dimension for SGMD is mostly determined to construct the trajectory matrix via the manual experience or power spectral density method. The manual determination of embedding dimension will introduce many uncertainties into the decomposition results of SGMD, thereby leading to some issues (e.g., the over-decomposition or under-decomposition). Additionally, it easily leads to the larger dimensions, the added decomposition components and the longer execution times via employing the power spectral density approach to determine the embedding dimension of SGMD. That said, when this method is used to select the embedding dimension, the curse of dimensionality and a lot of useless components are easily generated in the decomposition process of SGMD, thereby affecting the decomposition performance and operation efficiency of SGMD. Considering that the relative entropy can effectively calculate the discrepancy between probability distributions of two signals[18]. Therefore, to enhance the decomposition efficacy of conventional SGMD and overcome the shortcomings of manual selection of embedding dimension of traditional SGMD, this study presents a POSGMD for adaptive signal decomposition and obtaining several SGC, where the relative entropy is employed to automatically ascertain the optimal embedding dimension of SGMD. Meanwhile, considering that the contribution degree of fault information of each SGC is different, so the kurtosis-weighted principle is further introduced for signal reconstruction, which is aimed at more comprehensively utilizing fault information of each SGC and reducing the influence of the latent noise interference to a certain extent.

After signal decomposition and reconstruction,

many scholars used some classification models to extract fault features from the processed signals and intelligently identify fault types. The used common classification models comprise support vector machine (SVM), and back propagation neural network (BPNN), among others. However, these classification models belong to shallow models, and their recognition performance will sharply decline when faced with an increase in data volume. To deal with this problem, deep learning (DL) technology is proposed and rapidly developed by other scholars, which has been effectively implemented in bearing anomaly diagnosis[19-20]. Particularly, compared with other DL models (e.g., deep belief network (DBN) and autoencoder), CNN is deemed to be one more representative and prominent DL algorithm, which distinguished by its superior feature extraction capabilities, has garnered significant achievements in fault diagnosis[21-22]. Cheng et al.[23] suggested a sophisticated fault detection technique for rotating equipment utilizing a continuous wavelet transformation local binary CNN framework. Experimental results demonstrate its superiority in bearing faults and compound gearbox fault diagnosis. Xu et al.[24] proposed to enhance the InceptionNet through a combination of intrinsic feature extraction (IFE) and convolutional block attention module (CBAM). Their method offers a comprehensive approach to signal processing, culminating in the fault diagnosis process. Hu et al.[25] presented a fault diagnosis approach predicated on CNN. This approach addresses the complexities of signal processing and professional expertise in traditional fault diagnosis methods. He et al. [26] presented a fault diagnosis approach for flywheel energy storage system bearings utilizing parameter-optimized VMD and energy entropy.

The data imbalance in actual industrial scenarios constrains the application of deep learning fault diagnosis methods. To address this issue, many researchers have explored integrating dynamic model responses into training processes. Feng et al.[27] proposed a digital twin-driven intelligent health management method to monitor and assess gear surface degradation progression, enabling accurate remaining useful life (RUL) prediction and predictive maintenance decision-making. Ming et al.[28] introduced a digital twin-assisted framework to enhance rolling bearing fault diagnosis under imbalanced data by minimizing discrepancies between dynamic model responses and real measured data. Ni et al.[29] presented a novel Physics-Informed Residual Network (PIResNet), by integrating physical modal properties and a domain-conversion mechanism, the method demonstrates superior fault diagnosis performance under variable operating speeds and loads. Li et al.[30] introduced the FCZD-IA framework, a zero-sample diagnostic method using infrared thermography and acoustic data to enhance gearbox fault detection. It combines a neuro-fuzzy system and deep learning for robust, interpretable diagnostics, showing superior performance in experiments. Nevertheless, in the real environments with high levels of noise, traditional CNN model is prone to the gradient vanishing and over-fitting issues, thereby affecting its robustness and generalization capability. To address this concern, by replacing the original convolutional layers of traditional CNN with the convolutional blocks and residual blocks, this study proposes an ICNN for fault feature extraction and automatic recognition of bearing fault types.

Existing studies on fault diagnosis for wind turbine bearings have achieved notable progress, particularly with the integration of deep learning techniques. However, several research gaps remain to be addressed. Firstly, many conventional methods exhibit limited robustness to strong noise interference, leading to reduced fault identification accuracy in practical scenarios. Secondly, the model complexity of some deep learning-based approaches is high, which increases computational cost and limits their applicability in real-time industrial environments. Thirdly, many algorithms rely heavily on manually selected parameters, such as embedding dimensions or filter parameters, which may introduce subjectivity and reduce repeatability. In addition the emerging digital twin technology has shown great potential in fault diagnosis by bridging physical systems and virtual models. However, its application faces challenges such as high computational costs, reliance on domain knowledge for accurate modeling, and the need for substantial high-quality data,

In summary, to enhance the fault identification accuracy of wind turbine bearings under strong noise scenario, this paper presents an improved bearing fault diagnosis method derived from POSGMD and ICNN. Firstly, POSGMD is introduced to adaptively decompose the collected original bearing vibration signal into various SGC, where the embedding

dimension is automatically determined predicated on the relative entropy. Meanwhile, the signal reconstruction is performed based on kurtosis-weighted criteria to obtain the reconstructed signals. Subsequently, the CWT of the obtained reconstructed signals is calculated to generate the corresponding time-frequency images and execute dataset partitioning. Finally, the proposed ICNN is introduced for model training and automatic recognition of bearing faults. The efficiency and ascendancy of the presented approach are validated through the analysis of two experimental cases. The primary contributions of this study are encapsulated below:

1) By introducing the relative entropy and kurtosis-weighted principle into the original SGMD, a POSGMD is presented for adaptive signal decomposition and signal reconstruction, which can both avoid the problem of manual selection of embedding dimension of SGMD and mitigate the impact of strong noises to a certain degree.

2) By replacing the original convolutional layers of CNN with the convolutional blocks and residual blocks, an ICNN is introduced for automatic feature extraction and fault identification, which can both mitigate the over-fitting and address the gradient vanishing issue encountered during the training process of traditional CNN.

3) A cutting-edge bearing fault diagnostic methodology predicated on POSGMD and ICNN is proposed, which can enhance the fault diagnosis precision of bearings under noisy scenarios.

The ensuing sections of this paper are scheduled as the following aspects. Section 1 displays the related theory about POSGMD. Section 2 elaborates on the related theory about ICNN. Section 3 presents a inventive bearing fault diagnosis approach predicated on POSGMD and ICNN and introduces its realization process. Section 4 substantiates the efficacy and supremacy of the presented approach through two sets of experiments. Finally, Section 5 wraps up and discusses potential directions for additional research.

1 POSGMD

1.1 SGMD

SGMD is a phase space geometric analysis method that employs symplectic geometry similarity transformations to compute the eigenvalues of Hamiltonian matrix. It reconstructs SGCs utilizing the corresponding eigenvectors, facilitating the adaptive decomposition of non-stationary signals. Throughout the decomposition process, SGMD preserves the invariance of the original temporal sequence, demonstrating robust decomposition capabilities[31, 32]. The specific procedure of SGMD is outlined as follows:

1) Phase-space reconstruction. Assuming an input signal sequence as $x = x_1, x_2, \ldots, x_n$, where n represents the length of the signal data. Based on Takens embedding theory, we employ the method of delay to process one-dimensional signals. By doing so, it becomes possible to reconstruct multidimensional signals, resulting in the generation of a trajectory matrix $\boldsymbol{X}$.

$$\boldsymbol{X} = \begin{bmatrix} x_1 & \ldots & x_1 + (d-1)\tau \\ \ldots & \ldots & \ldots \\ x_m & \ldots & x_m + (d-1)\tau \end{bmatrix} \tag{1}$$

where d denotes the dimensionality of the embedding, τ stands for the delay time, and $m = n - (d-1)\tau$. To ensure the rationality of reconstructing the matrix $\boldsymbol{X}$, d is generally selected predicated on the power spectral density (PSD) of the input signal x.

2) Symplectic geometric matrix transformation. The covariance matrix $\boldsymbol{A}$ is created as $\boldsymbol{A} = \boldsymbol{X}^{\mathrm{T}}\boldsymbol{X}$, which results in the Hamiltonian matrix $\boldsymbol{M}$.

Then, if $\boldsymbol{F} = \boldsymbol{M}^2$, the matrix $\boldsymbol{F}$ also becomes a Hamiltonian matrix, which can be acquired by using the symplectic orthogonal matrix $\boldsymbol{Q}$.

$$\boldsymbol{Q}^{\mathrm{T}}\boldsymbol{F}\boldsymbol{Q} = \begin{bmatrix} \boldsymbol{B} & \boldsymbol{R} \\ 0 & \boldsymbol{B}^{\mathrm{T}} \end{bmatrix} \tag{2}$$

where $\boldsymbol{B}$ is an upper triangular matrix with elements $b_{ij} = 0 (i > j+1)$. By computation, the eigenvalues of $\boldsymbol{B}$ are $\lambda_1, \lambda_2, \ldots, \lambda_d$. Hence, the eigenvalues of $\boldsymbol{A}$ are represented as $\sigma_i = \sqrt{\lambda_i}$. Correspondingly, the associated eigenvectors are $\boldsymbol{Q}_i$. Let $\boldsymbol{S} = \boldsymbol{Q}^{\mathrm{T}}\boldsymbol{X}, \boldsymbol{Z} = \boldsymbol{Q}\boldsymbol{S}$. Derived from a sequence of initial single-component matrices $\boldsymbol{Z}_i$, the reconstructed trajectory matrix $\boldsymbol{Z}$ is meticulously crafted, such that $\boldsymbol{Z} = \boldsymbol{Z}_1 + \boldsymbol{Z}_2 + \ldots + \boldsymbol{Z}_d$. Here, $\boldsymbol{Z}_i = \boldsymbol{Q}_i\boldsymbol{S}_i$ and $\boldsymbol{S}_i = \boldsymbol{Q}_i^{\mathrm{T}}\boldsymbol{X}^{\mathrm{T}}$.

Finally, the diagonal average results of d component signals are expressed as $\boldsymbol{Y} = \boldsymbol{Y}_1 + \boldsymbol{Y}_2 + \ldots + \boldsymbol{Y}_d$.

1.2 POSGMD

SGMD is an adaptive signal analysis algorithm. However, the embedding dimension of traditional SGMD is selected by using manual experience or the power spectral density method of the input signal, which exerts a substantial influence on its decomposition performance. Specifically, if the

embedding dimension is set as too large, too many unimportant components may be obtained to generate the over-decomposition problem and lengthy processing time. On the contrary, if the embedding dimension is set as too small, some useful components might be lost to result in the under-decomposition problem. Henceforth, in order to deal with this problem, this study suggests a POSGMD via using the relative entropy to automatically determine the embedding dimension in the decomposition process. Different from traditional SGMD, the proposed POSGMD includes both adaptive signal decomposition and signal reconstruction process, which is aimed at reducing the interference of strong noises in the original signal. Fig.1 illustrates the flowchart of the parameter-optimized SGMD.

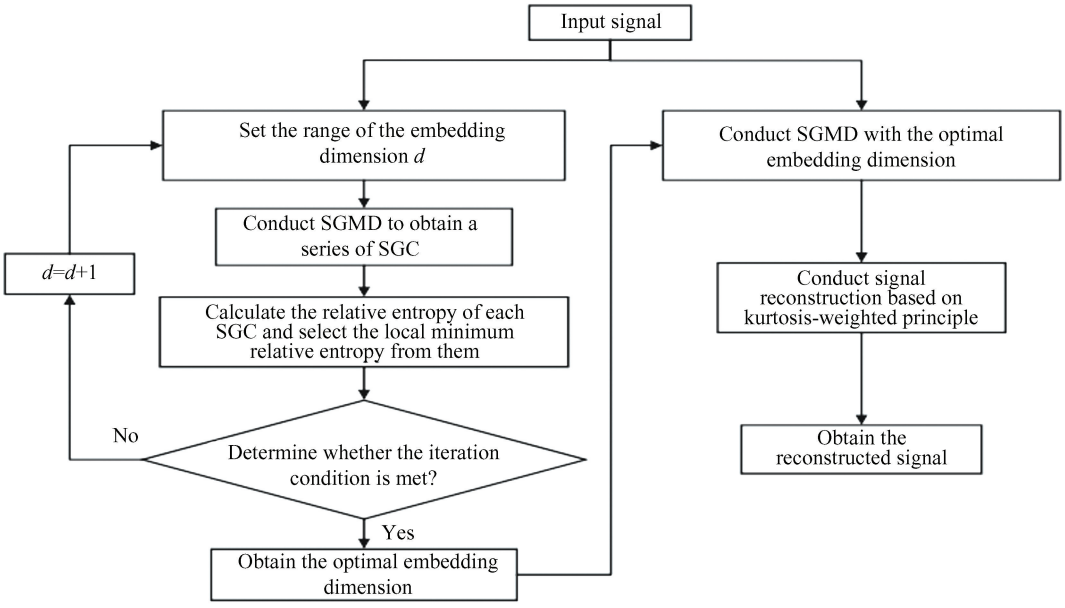

Fig.1 The flowchart of POSGMD method

The precise steps involved in POSGMD are outlined below:

1) Load the collected bearing vibration signals and initialize the range of embedding dimension d of SGMD, and d is empirically chosen within the range of 2 to 10. In this step, the decomposition efficacy and computational efficiency in a holistic manner are thoroughly evaluated.

2) SGMD is adopted to disassemble the initial signal into a sequence of SGCs.

3) Calculate the relative entropy of each SGC obtained from SGMD and select the smaller relative entropy from them as the local minimum relative entropy. In this step, the relative entropy of each SGC obtained by SGMD can be calculated by the following equation[33]:

$$K_L(P \,||\, Q) = \sum P(y_i) \log \frac{P(y_i)}{Q(y_i)} \tag{3}$$

where K_L is the relative entropy, which is the difference in information entropy between two probability distributions, y_i is the i-th SGC, $P(y_i)$ and $Q(y_i)$ represent two probability distributions of the i-th SGC. In this step, the bigger relative entropy implies a greater difference between the decomposed component and the actual component (i.e., the worse the decomposition results), whereas the smaller relative entropy means a greater similarity between the decomposed component and the actual component (i.e., the better the decomposition performance). Therefore, the optimal embedding dimension of SGMD is adaptively determined based on minimum relative entropy.

4) Ascertain whether the iteration condition is met. In particular, if the largest embedding dimension is achieved, stop the iterative process, select the smallest value from all local minimum relative entropy as global minimum relative entropy, and output the embedding dimension corresponding to global minimum relative entropy as the optimal embedding dimension of SGMD. Otherwise, set $d = d + 1$, go back to Step 1) and carry out the iterative procedure again until the stop condition is met.

5) SGMD with the optimal embedding

dimension d_0 is used to decompose the signals into various SGC.

6) The kurtosis-weighted principle is introduced for adaptive signal reconstruction. Specifically, in this step, the correlation kurtosis of each SGC is firstly calculated by the following equation:

$$K_{\mathrm{ck}}(T_{\mathrm{s}}) = \frac{\sum_{n=1}^{N}\prod_{m=0}^{M} y_{n-mT_{\mathrm{s}}}}{\left(\sum_{n=1}^{N} y_n^2\right)^{M+1}} \tag{4}$$

where K_{ck} is the correlation kurtosis, N is the number of samples in the input signal, n is the n-th SGC, T_{S} is the deconvolution period and M denotes the displacement factor. Then, the kurtosis-weighted sum of all SGC is conducted to acquire the final reconstructed signal, which can be represented by

$$x_{\mathrm{re}} = \sum_{i=1}^{d_o} \gamma_i S_{\mathrm{SGC}_i} = \sum_{i=1}^{d_o} \frac{K_{\mathrm{ck}i}}{\sum_{i=1}^{d_o} K_{\mathrm{ck}i}} S_{\mathrm{SGC}_i} \tag{5}$$

where $x_{\mathrm{re}}(t)$ is the reconstructed signal, d_{o} is the number of SGCs, γ_i is the weighting coefficient of the i-th SGC, $K_{\mathrm{ck}\,i}$ indicates the correlation kurtosis of the i-th SGC, and $S_{\mathrm{SGC}\,i}$ means the i-th SGC.

2 ICNN

2.1 Traditional CNN

CNN is an effective deep learning model and can extract automatically fault characteristics from the raw signal, which has been used in several tasks (e.g., image classification, object detection and fault diagnosis). CNN is mainly comprised of convolutional layers, max pooling layers, and fully connected layers. Firstly, the original signal is input into the convolutional layers with a batch normalization and using rectified linear unit (ReLU) as the activation function, where the convolutional operations with different size of kernels are used to extract local features from the source signal. Then, the features obtained by convolutional layers are fed into max pooling layers, where the downsample operations are performed to screen some important features and reduce the parameter quantity. Finally, the fully connected layers are combined with softmax for classify the extracted features from the previous layer.

2.2 ICNN

When the local faults occur in rolling bearings, the fault-related information embedded in bearing vibration signals often gets submerged within high levels of noises. When traditional CNN is used to handle bearing vibration signals in high-noise scenarios, their feature learning capability tends to decline. Simultaneously, traditional CNN is prone to the over-fitting and gradient vanishing issues when dealing with noisy signals, thereby easily affecting their generalization ability. To address the shortcomings of traditional CNN and ameliorate fault identification precision under noisy scenario, this research presents an ICNN model. Fig.2 depicts the architecture of the presented ICNN, where its two pivotal blocks (i.e., the convolution block and residual block) are displayed in Fig.3.

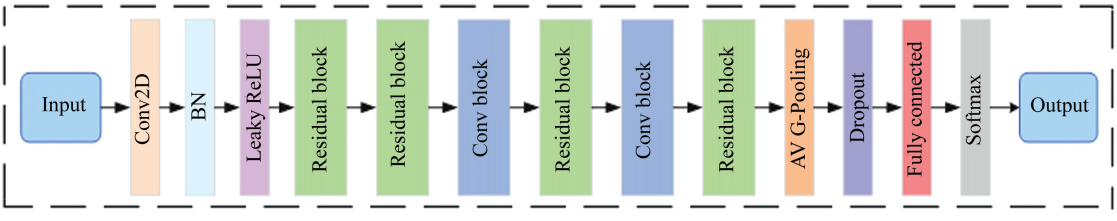

Fig.2 Architecture of ICNN model

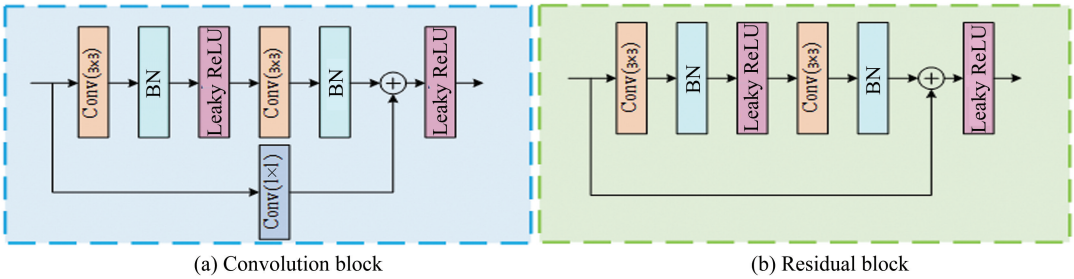

(a) Convolution block (b) Residual block

Fig.3 Convolution block and residual block

The following is a description of the specifics of the proposed ICNN:

1) Firstly, the input signal is fed into a convolutional layer with a 3×3 kernel size for conducting the initial feature extraction. Meanwhile, after being batch-normalized, the collected features are passed into an activation function named Leaky ReLU to enhance the non-linear expressive capability of network model.

2) Subsequently, the features extracted from the first convolutional layer are passed into two residual blocks and two convolutional-residual block units for enhancing feature learning and alleviating the vanishing gradient issue, where each convolutional-residual block unit includes a convolutional block (as highlighted in blue in Fig.2) and a residual block (as highlighted in green in Fig.2). Specifically, as shown in Fig.3, each residual block has two branches, with two convolutional layers on one branch, two batch normalization layers, and one Leaky ReLU activation layer, whereas another branch (the residual branch) involves a skip connection. Different from the residual block, the residual branch of each convolutional block is not directly connected, but rather connected by a convolutional layer with the kernel size of 1×1. After deep feature learning, one global average pooling layer is used to further decrease the feature parameters and improve computing efficiency. Additionally, to mitigate the over-fitting problem, a dropout layer is additionally incorporated to discard the outputs from a portion of neurons.

3) Finally, the extracted feature maps from global average pooling layer are transformed into the final classification output by using the fully connected layer. Meanwhile, Softmax function is employed to convert each fault category into its corresponding probability, thereby determining the class label based on probability distribution and achieving fault identification.

In the proposed ICNN, due to the Leaky ReLU represents an enhanced iteration of ReLU activation function, which can not only address the gradient vanishing problem associated with the sigmoid activation function but also mitigate the problem of the deactivation of certain neurons caused by zeroing out the input in ReLU. Therefore, this study selects the Leaky ReLU as the activation function of the ICNN, which can be defined as stated below:

$$h^{(i)} = \max(w_i x, 0) = \begin{cases} w_i x, & w_i x > 0 \\ a w_i x, & \text{else} \end{cases} \tag{6}$$

where α is set as 0.2, which is used to ensure a slight output when the input is less than 0.

In the training process of the presented ICNN, the difference between the actual labels and projected outputs is measured using the cross-entropy loss function. Besides, the Adam optimizer is utilized to renew the parameters of network model, thereby minimizing the loss function and enhancing the learning efficacy of network. Compared with the traditional CNN, the proposed ICNN model, with enhanced convolutional blocks and residual blocks, effectively mitigates the gradient vanishing issue during training. Additionally, in the proposed ICNN, the inclusion of batch normalization (BN) layers and dropout layers will contribute to enhance the model's anti-noise capacity and prevent the network's over-fitting.

3 POSGMD and ICNN-based Rolling Bearing Fault Diagnostic Method

This study suggests a novel rolling bearing fault diagnostic technique predicated on POSGMD and ICNN to increase fault detection accuracy in noisy scenarios, which mainly involves three procedures (i.e., vibration signal acquisition, signal decomposition and reconstruction, and bearing intelligent fault diagnosis). Fig.4 depicts the flowchart of the presented fault diagnosis approach.

The following are the exact phases of the presented fault diagnostic approach:

1) Vibration signal acquisition. In this step, one accelerometer is installed on bearing fault simulation test bench, and a data acquisition card is utilized to gather vibration signals from bearings under various fault situations.

2) Signal decomposition and reconstruction. Firstly, POSGMD is initially adopted to decompose the gathered original bearing vibration signal into a string of SGC, where the optimal embedding dimension is adaptively determined with the help of the relative entropy. Subsequently, based on kurtosis-weighted criterion, the weighted sum of the obtained SGC are conducted to obtain the reconstructed signal. Finally, the CWT of the reconstructed signals is computed to generate the corresponding time-frequency images. Meanwhile, the received images are proportionally divided into the sample set (i.e., the training set, validation set and testing set) at a proportion of 7∶1∶2 by using random segmentation technique.

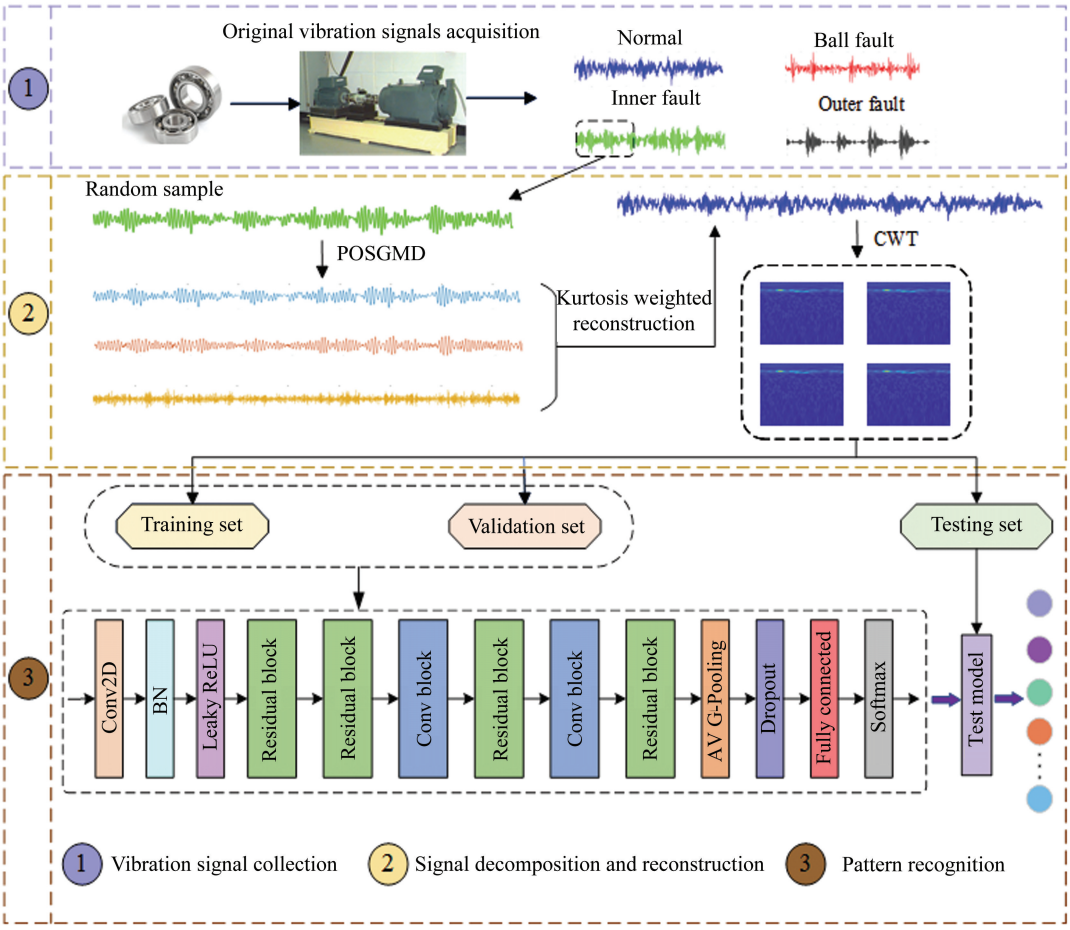

Fig. 4 Flowchart of the proposed bearing fault diagnosis method

3) Bearing intelligent fault diagnosis. In this step, the training and validation sets are fed into the presented ICNN for network model training and parameter tuning, whereas the testing set is fed into the well-trained ICNN model for model testing, thereby automatically outputting the results.

4 Experimental Verification

In this segment, two experimental cases were undertaken to verify the superiority and applicability of the presented approach in bearing fault identification under noise scenarios. The experiments were conducted on a PC platform running a version of Windows 10, equipped with an Intel Core™ i5-8300H CPU@2.30GHz, 16GB of memory. The utilized software for the experiments is Matlab 2020b version.

4.1 Case 1: Bearing Fault Diagnosis of CWRU Data

4.1.1 Introduction to the benchmark dataset

The Case Western Reserve University (CWRU) bearing data centre dataset was used to verify the efficacy of the the presented approach. Fig. 5 illustrates the schematic diagram of the experimental setup, which primarily comprises a motor, test bearings, and power measurement instruments. In this experiment, in order to simulate bearing local faults, the electric discharge machining (EDM) was employed to create three different diameters of faults (i.e., 0.007 inches, 0.014 inches and 0.021 inches) on the surfaces on the inner race (IR), outer race (OR), and ball (RB) of normal bearings. In the data collection process, the motor speed was set at 1797 r/min, with a sampling frequency of 48 kHz, and one accelerometer was mounted on the drive end of the test bearing (model: 6205-2RS JEM SKF) to collect the bearing vibration signals. Altogether 10 different operational conditions of bearing vibration signals were gathered, comprising 9 different fault states and one normal state. Table 1 provides detailed information on the sample dataset of testing bearings. Additionally, the collected data samples are randomly partitioned into training, validation, and testing sets

at a ratio of 7∶1∶2. The time-domain waveform of a single sample under ten various operational scenarios is presented in Fig. 6. It can be observed from Fig. 6, as a result of the interference of noises, there is a certain similarity between different signal waveforms, making it challenging to accurately determine the type of bearing defects by direct signal waveform observation.

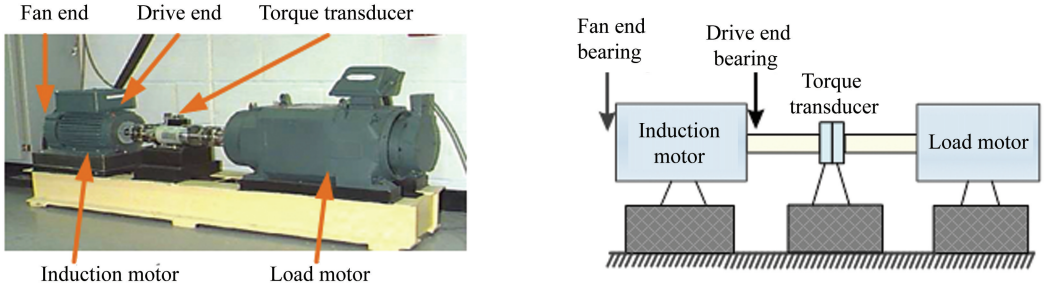

(a) Bearing fault simulation experimental device (b) The structure diagram

Fig.5 Bearing fault simulation experimental device and its structure diagram

Table 1 Sample information of bearing vibration data in Case 1

Class label	Bearing status	Fault diameter	Data length	Number of samples	Rotational speed(r/min)
1	BF7	0.007	2048	100	1797
2	BF14	0.014	2048	100	1797
3	BF21	0.021	2048	100	1797
4	IRF7	0.007	2048	100	1797
5	IRF14	0.014	2048	100	1797
6	IRF21	0.021	2048	100	1797
7	ORF7	0.007	2048	100	1797
8	ORF14	0.014	2048	100	1797
9	ORF21	0.021	2048	100	1797
10	Normal	0	2048	100	1797

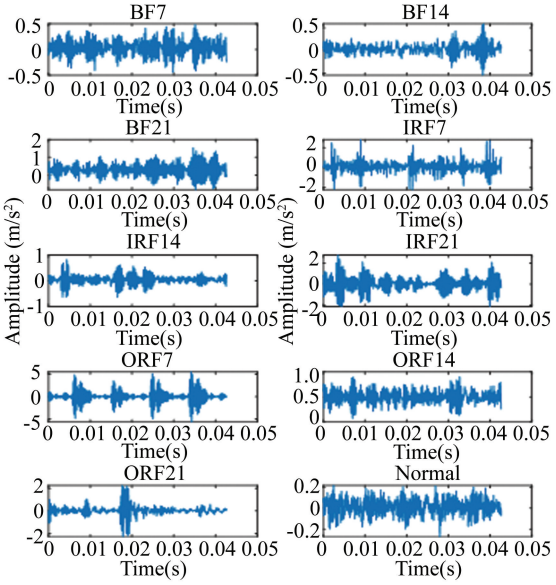

Fig.6 Time-domain waveform of one sample under different bearing working states in Case 1

4.1.2 Fault diagnosis results of the proposed method

To effectively distinguish bearing fault categories, the proposed method is applied to analyze the dataset from CWRU. In accordance with the flowchart in Fig.4, POSGMD is initially employed to disassemble the initial bearing vibration signal into multiple SGC, where the embedding dimension is automatically chosen by using the relative entropy. Meanwhile, based on the kurtosis-weighted principle, signal reconstruction is conducted to acquire the reconstructed signals. Secondly, CWT of the reconstructed signals is calculated to acquire the corresponding time-frequency images as sample set. Finally, the proposed ICNN is introduced for autonomous feature extraction and fault identification. Table 2 lists the model parameters of the proposed ICNN. Fig.7 illustrates the network training curve and loss curve of the proposed ICNN. As shown in Fig.7, when the training iterations are larger than 100, the training accuracy can reach a stable value of 100%, whereas the training loss steadily decreases to zero. This indicates that the proposed ICNN model is well-trained. Fig.8 presents the confusion matrix acquired by the proposed approach. As displayed in Fig. 8, none of the samples are misidentified, and the suggested approach can get 100% identification accuracy. This outcome provides preliminary evidence for the proposed bearing fault diagnosis method's efficacy.

Table 2 Model parameters of the proposed ICNN

Layer	Type	Parameters	Output size
Input	Image input	–	64×64×3
Conv1	2D convolution	Kernel size: [3,3]; kernel number: 16; stride: [1,1]	64×64×16
BN1	Batch normalization	Epsilon: 1.0e-05	–
LReLU	Leaky ReLU	Scale: 0.2	–
Res1	Residual block	Kernel size: [3,3]; kernel number: 16; Stride: [1,1]; Epsilon: 1.0e-05; Scale: 0.2	–
Res2	Residual block	Kernel size: [3,3]; kernel number: 16; Stride: [1,1]; Epsilon: 1.0e-05; Scale: 0.2	64×64×16
Conv2	Conv block	Kernel size: [3,3]; kernel number: 16; Stride: [1,1]; Epsilon: 1.0e-05; Scale: 0.2	–
Res3	Residual block	Kernel size: [3,3]; kernel number: 16; Stride: [1,1]; Epsilon: 1.0e-05; Scale: 0.2	64×64×32
Conv3	Conv block	Kernel size: [3,3]; kernel number: 16; Stride: [1,1]; Epsilon: 1.0e-05; Scale: 0.2	–
Res4	Residual block	Kernel size: [3,3]; kernel number: 16; Stride: [1,1]; Epsilon: 1.0e-05; Scale: 0.2	64×64×64
Gapool	2D global average pooling	Kernel size: [8,8]; Stride: [1,1]	1×1×64
Dropout	Dropout	Probability: 0.20	1×1×64
FC	Fully connection	–	1×1×10
Softmax	Softmax	–	1×1×10
Classoutput	Classified output	–	–

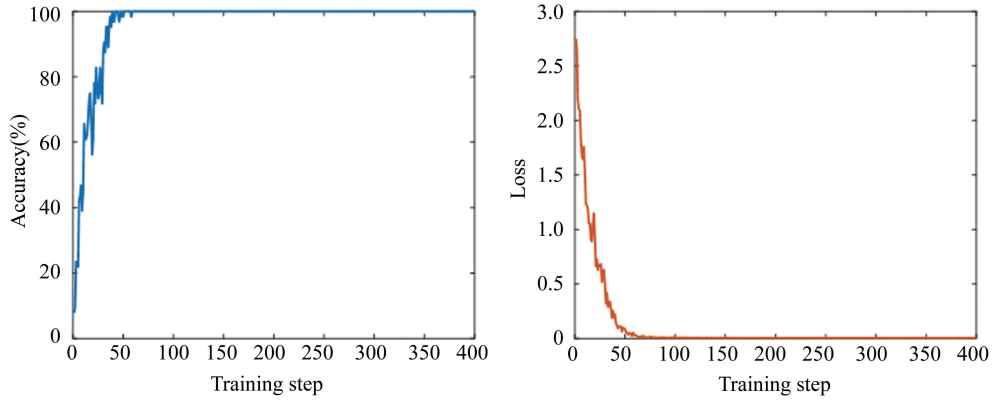

Fig.7 The training accuracy curve and loss curve of the proposed method in Case 1

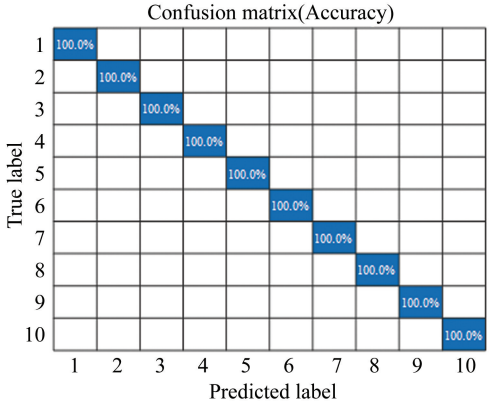

Fig. 8 Confusion matrix obtained by the proposed method in Case 1

4.1.3 Analysis of ablation experiments

To demonstrate the efficacy of POSGMD employed in the presented approach, we executed the comparisons between the proposed POSGMD with four similar methods (i. e., SGMD, ITD, EWT and CEEMD). In this comparison, all decomposition methods are used for processing the same experimental data. To ensure that these comparisons are equitable, in all signal decomposition methods, the kurtosis-weighted principle is also conducted for signal reconstruction. Besides, due to mechanical equipment in actual engineering often operates at noisy environments, so the Gaussian white noises with varying signal-to-noise ratio (*SNR*) are artificially

inserted into the experimental data for simulating the noisy data under different levels of noises, and then all methods are adopted to analyze these noisy data and identify bearing fault types under different levels of noises. Particularly, Gaussian white noises with $SNR = -6\text{dB}\ -6\text{dB}$ are inserted into the original signal, and the SNR can be computed by

$$SNR = 10\log\left(\frac{P_{\text{signal}}}{P_{\text{noise}}}\right) \tag{7}$$

where P_{signal} and P_{noise} stand for the average power of the actual bearing vibration signal and the Gaussian white noise, respectively.

Fig.9 displays the fault diagnosis results acquired by different decomposition approaches. It is apparent that the identification accuracy of different decomposition approaches will increase with the increase of SNR, as shown in Fig.9. Nevertheless, the proposed POSGMD can reach better recognition results compared with other decomposition approaches in scenarios with or without noise addition. Specifically, the discernment precision of the proposed POSGMD is evidently superior to that of alternative decomposition methodologies, particularly for a low $SNR = -6\text{dB}$. Therefore, the comparison results mean that the proposed POSGMD is adopted for signal decomposition and reconstruction, which is more reasonable and effective for bearing fault diagnosis.

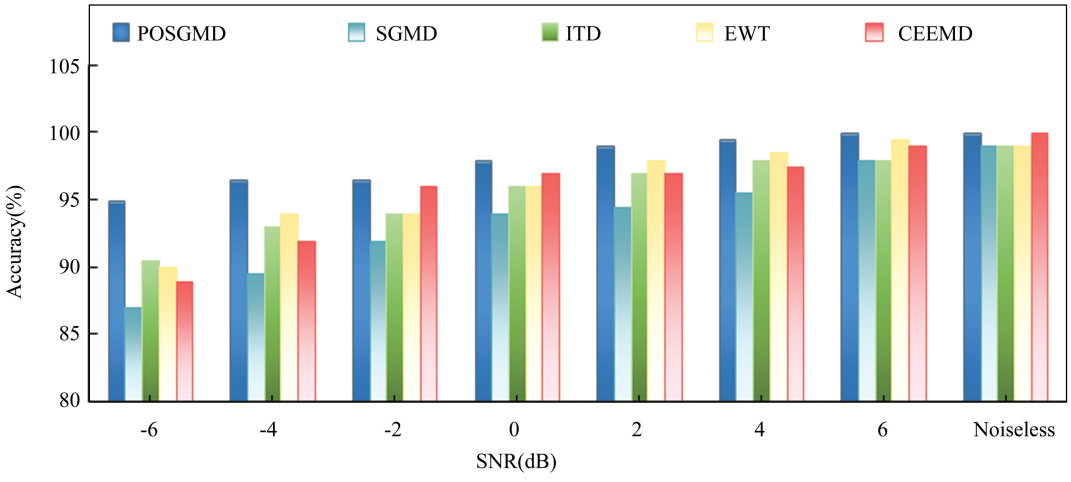

Fig. 9 Fault identification accuracy of different decomposition methods in Case 1

To demonstrate the feasibility and efficacy of the ICNN utilized in the proposed approach, we also conducted the comparisons between the presented ICNN with four standard classification models (i.e., CNN, LeNet5, AlexNet and ResNet). Concretely, in this comparison, all classification models are combined with POSGMD to extract fault features from the same experimental data and achieve fault classification. Namely, except for the classification model, the proposed procedure and the other processes are the same. The results of several classification models' fault identification at various noise levels are displayed in Fig.10. Similarly, as presented in Fig.10, when noises or no noises are inserted to the original signal, the identification accuracy of the presented ICNN model is all greater than that of other classification models. Particularly, when SNR is set as -6 dB, there is a greater difference in the identification precision between the presented ICNN with other classification models. Hence, this comparison results demonstrated the advantage of the presented ICNN model in identifying different types of bearing faults. In order to verify the advantages of the model used in this article in terms of time consumption and complexity, ICNN was compared with several typical deep learning models. Table 3 shows that ICNN has certain advantages in training time, significantly shorter than other methods, and has a much smaller total number of model parameters than CNN, LeNet5, and Alexnet.

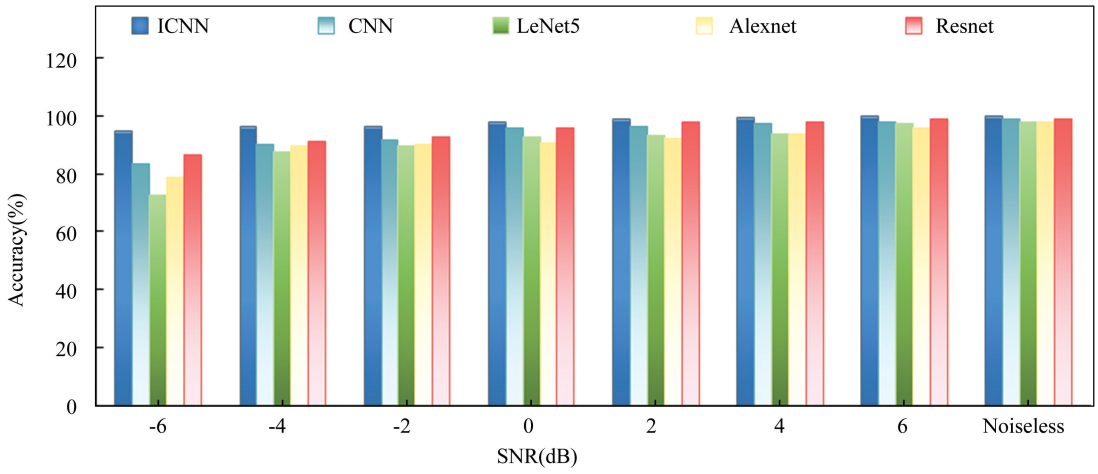

Fig.10 Fault identification accuracy of different classification models in Case 1

Table 3 Comparison of time consumption and complexity

Methods	Model parameter quantity	Training duration(s)
ICNN	227018	31
CNN	529578	45
LeNet5	390071	40
Alexnet	58322314	132
Resnet	169978	38

4.1.4 Comparative analysis with other representative fault diagnosis methods

To verify the efficacy and advantage of the presented approach in bearing fault identification, several typical fault diagnosis approaches (i. e., CEEMD-SVM, CNN-LSTM, CWT-CNN, WDCNN, DACNN and MCMS-CNN) are selected for conducting comparative analysis. Table 4 lists the specific details of six comparison approaches. Besides, the model parameters of these comparison methods are the same as the corresponding literature in Table 4. Similarly, all fault diagnosis methods are used for analyzing the same experimental data. Fig. 11 displays the identification results of different fault diagnosis methods under various levels of noises. As evidenced by Fig.11, as the noise intensity increases, the fault discernment precision of the presented approach and other fault diagnosis approaches has a downward trend. However, whether the noiseless addition or noise addition condition, the presented approach can all achieve the superior identification precision than other approaches. Even at a *SNR* of −6 dB, the proposed method can also accomplish the recognition accuracy of 95%, Compared with other methods, the accuracy rate is at least 10% higher. Therefore, it can be inferred from this comparative analysis that the proposed method exhibits higher robustness to noise interference compared with some emblematic approaches in identifying bearing fault types under strong noise conditions.

Table 4 Detailed description of several comparison methods

Methods	Descriptions	References
CEEMD-SVM	This method combines the CEEMD and SVM to assess the health states of rolling bearings.	Lu et al.[34]
MCNN-LSTM	In this method, multiscale convolutional neural networks (MCNN) with different kernel sizes are firstly used to automatically extract features from the original data, and then bearing fault types are recognized based on the learned features using long-short term memory (LSTM).	Chen et al.[35]
CWT-CNN	In this method, the CWT is firstly adopted to obtain the time-frequency characteristics from the original signal, and then CNN is introduced for automatic fault identification.	Tang et al.[36]
WDCNN	In this method, a deep convolutional network model (WDCNN) is presented for feature learning and fault identification, the first convolutional layer uses a broad convolutional kernel to reduce high-frequency noise and extract information.	Zhang et al.[37]
DACNN	In this method, a one-dimensional convolutional neural network model is proposed to solve the problem of accurate fault diagnosis of induction motor bearing under noise interference conditions.	Jia et al.[38]
MCMS-CNN	In this method, a multichannel multiscale convolutional neural network (MCMS-CNN) is proposed, which can automatically learn complementary and rich features at different scales, better extracting fault information.	Xu et al.[39]

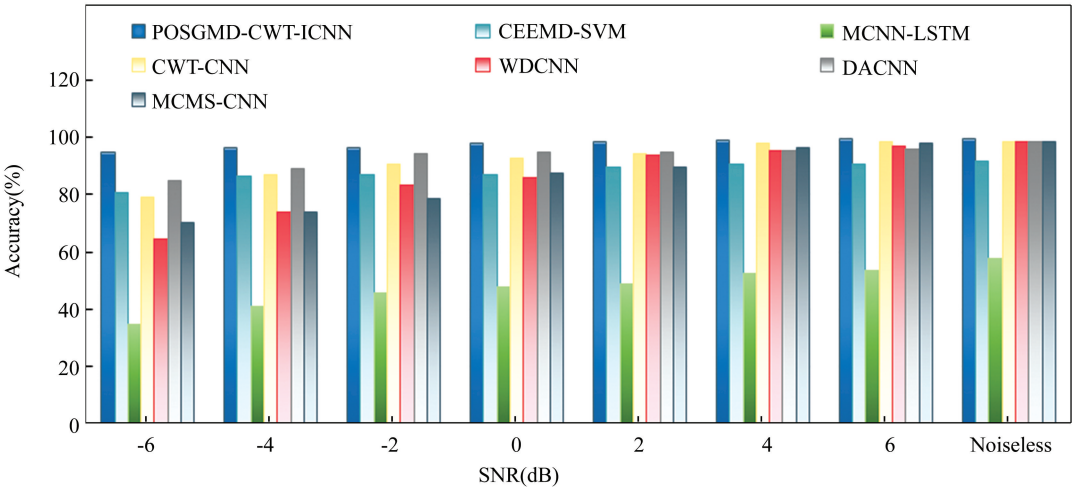

Fig.11 Comparative analysis results of different fault diagnosis methods in Case 1

4.2 Case 2: Bearing Fault Diagnosis of Laboratory Data

4.2.1 Introduction to the experimental dataset

Bearing fault data utilized in this experiment are collected from the ABLT-1A experimental equipment at Southeast University (SEU), which is comprised of a computer control system, test head, lubricating system, conveyance system, loading system, motor control system, and data collection system, as depicted in Fig. 12. The motor control system is used to adjust the motor speed, whereas the loading system is adopted to apply the force on testing bearing. The type of testing bearings is HRB6205. In this experiment, the collected entire dataset consists of seven bearing working states (i.e., normal, outer race fault (ORF), inner race fault (IRF), ball fault (BF), outer-inner race compound fault (OIF), outer race and ball compound fault (OBF), and outer-inner race-ball compound fault (OIBF). These bearing faults have 1 mm width, which are induced by applying electrical discharge machining (EDM). In data collection, two PCB-based accelerometers (Sensor-1 and Sensor-2) are firstly installed on the vertical direction of bearing housing, and then the NI9234 data acquisition card is connected with the accelerometer to record bearing vibration signal. The motor load is set as 5.1 kN, and the rotating speed and sampling frequency are designate as 1050 r/min and 12 kHz, respectively. Table 5 presents the sample information of bearing vibration data. Altogether 700 samples are collected, which are randomly segmented into training, validation, and testing sets at a proportion of 7∶1∶2. The time-domain waveform of a single sample under different bearing operating conditions is shown in Fig.13. As shown in Fig.13, owing to the noise interference and the similarity of time-domain waveform under different bearing operating states, by looking at time-domain waveforms directly, bearing fault types are hard to discern. Therefore, it is imperative to embrace an efficacious approach for extracting the useful feature information and achieving automatic identification of bearing faults.

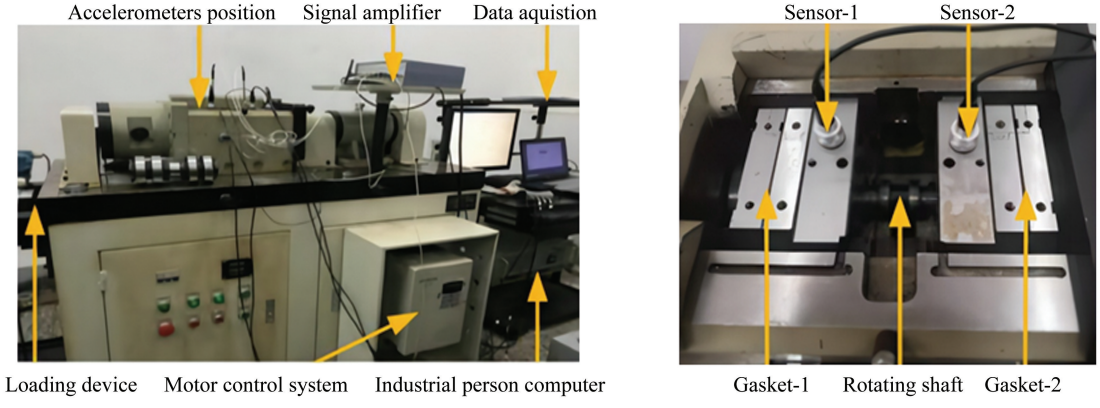

Fig.12 ABLT-1A experimental equipment

Table 5 Sample information of bearing vibration data in Case 2

Class label	Bearing status	Data length	Number of samples	Rotational speed (r/min)
1	Normal	2048	100	1050
2	ORF	2048	100	1050
3	IRF	2048	100	1050
4	BF	2048	100	1050
5	OIF	2048	100	1050
6	OBF	2048	100	1050
7	OIBF	2048	100	1050

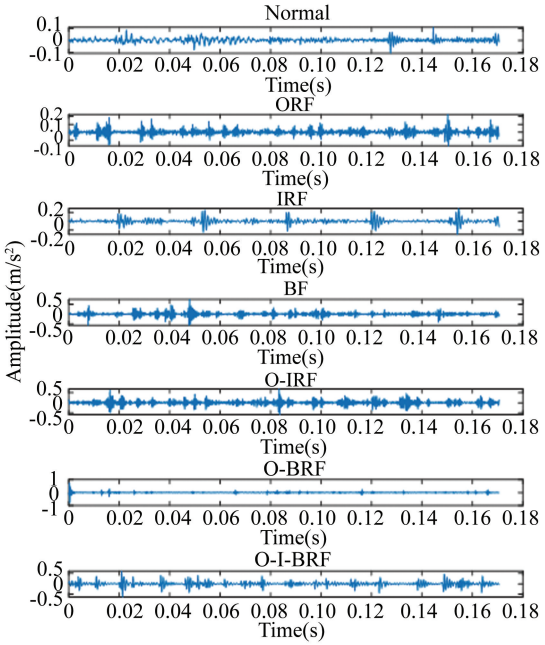

Fig.13 Time-domain waveform of one sample under different bearing working states in Case 2

4.2.2 Fault diagnosis results of the proposed method

To showcase the availability of the presented method, the method is utilized to analyze the bearing dataset from Case 2. In this case, except for the parameters set to kernel number (7) in the fully connected layer, other model parameters of the presented ICNN are the identical to that of Case 1. Fig.14 shows the network training curve and loss curve of the proposed ICNN. As shown in Fig.14, the presented ICNN can achieve a training precision of 100% and a loss value close to zero, when the training iterations are bigger than 100. Fig.15 plots the confusion matrix acquired by the presented approach. As presented in Fig.15, the identification precision of the presented method is 100% for each bearing fault categories, which shows that various bearing faults may be properly identified using the proposed method. To rephrase, the presented method's efficacy are preliminarily verified.

4.2.3 Analysis of ablation experiments

Equal to Case 1, to display the validity and reasonability of POSGMD adopted in the proposed approach, the performance comparisons between the presented POSGMD with four similar decomposition approaches (i.e., SGMD, ITD, EWT and CEEMD) are also conducted under different noise levels. Fig.16 shows fault identification results of various signal decomposition approaches. It is evident from Fig.16 that identification accuracy of all decomposition methods will decrease as the *SNR* decreases. When *SNR* is bigger than 2 dB, for the presented POSGMD and other decomposition approaches, there is no significant difference in accuracy. However, when *SNR* is less than −2 dB, the recognition precision of the proposed POSGMD far exceeds that of alternative decomposition approaches. Even at −6 dB, the proposed method can additionally attain a recognition precision of 95%. Therefore, this comparison results illustrate the advantages of the presented POSGMD over decomposition approaches and the reasonability of using POSGMD method for signal processing in this study.

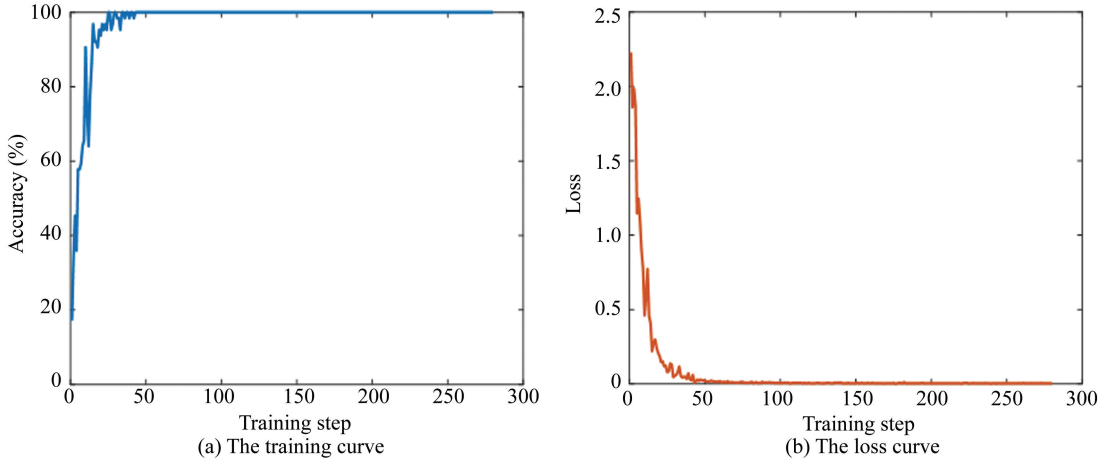

Fig.14 The training accuracy curve and loss curve of the proposed method in Case 2

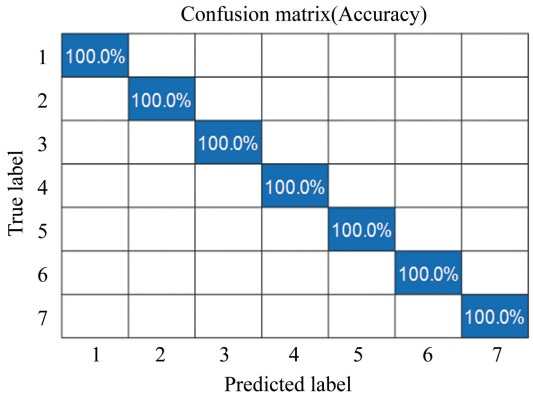

Fig.15 Confusion matrix obtained by the proposed method in Case 2

Equally, to present the efficacy and feasibility of ICNN applied in the presented method, the performance comparisons between the ICNN with four standard classification approaches (i. e., CNN, LeNet5, AlexNet and ResNet) are also conducted under different noise levels. Fig.17 plots the fault identification results of various classification models. As depicted in Fig.17, the proposed ICNN model has high accuracy under different *SNR*. Particularly, when SNR is less than −2 dB, the presented ICNN can still achieve the identification precision of 94% above, which is evidently superior to other classification approaches. Therefore, this comparative results further substantiate the efficacy and advantage of the presented ICNN for bearing fault identification under noisy conditions.

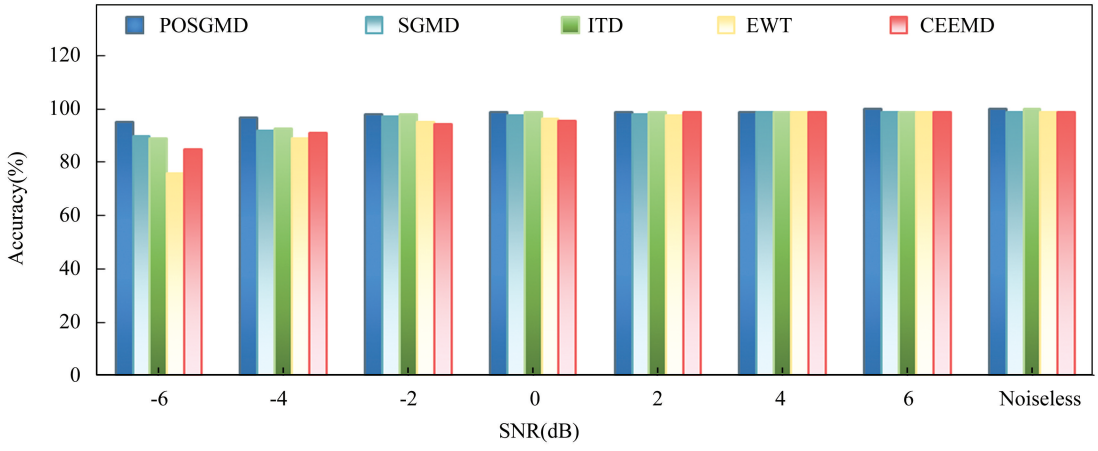

Fig.16 Fault identification accuracy of different decomposition methods in Case 2

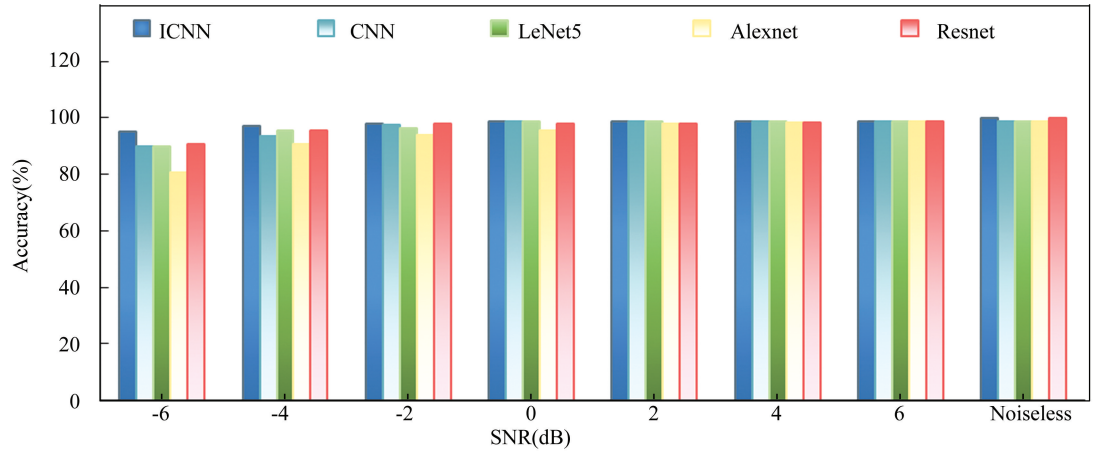

Fig.17 Fault identification accuracy of different classification models in Case 2

4.2.4 Comparative analysis with other similar fault diagnosis methods

Equal to Case 1, to display the availability and advantage of the presented approach in bearing fault identification, the presented approach is compared with other several typical fault diagnosis approaches (i. e., CEEMD-SVM, CNN-LSTM, CWT-CNN, WDCNN, DACNN and MCMS-CNN). Fig.18

displays the fault identification results of various fault diagnosis methods. As illustrated in Fig.18, when *SNR* is larger than −2 dB, identification precision of the presented approach is relatively close to that of CWT-CNN. However, when *SNR* is lower than −2 dB, the presented approach has a greater identification precision, particularly for *SNR* = −6 dB. Besides, whether the noiseless addition or noise addition condition (e.g., *SNR* rangs from −6 dB to 6 dB), compared with the other fault diagnostic approaches, the suggested method's accuracy in fault detection appears to be greater. Consequently, from this comparative result, we can additionally infer that the presented approach behaves better in bearing fault identification than other several fault diagnosis approaches in strong noise scenarios.

4.3 Future Research Discussion

Via the aforementioned comparative analysis with various fault diagnosis methods, this study demonstrates the efficacy and advantage of the presented approach in bearing fault diagnosis. However, there are still some areas worth further research in the presented method, it can be summed up as stated below:

First and foremost, despite the proposed POSGMD can be suitable for processing one-dimensional non-stationary signal, it is currently unable to synchronously process multi-channel signals. Therefore, in our future work, illuminated by the idea of multi-channel signal analysis in multivariate empirical mode decomposition (MEMD), POSGMD will be further extended to the field of multi-channel signal analysis.

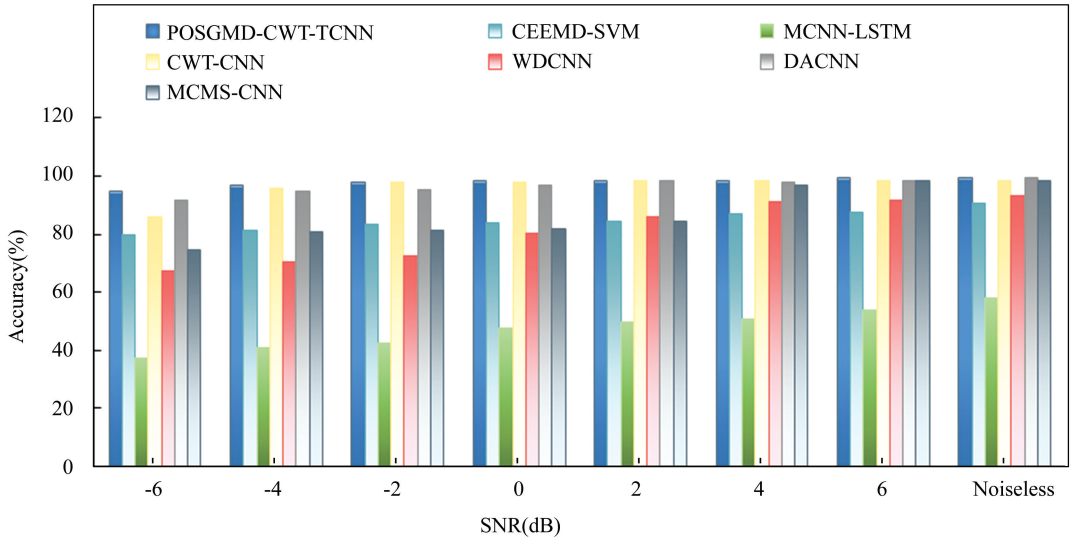

Fig.18 Comparative analysis results of different fault diagnosis methods in Case 2

Secondly, although the presented ICNN can efficiently extract fault feature information in noisy environments and accomplish fault discrimination, its model parameter settings have manual experience. Consequently, in our upcoming work, to avoid the manual selection of model parameters in the presented ICNN, some recently advanced optimizers (e.g., dung beetle optimizer (DBO), pelican optimization algorithm (POA), rat swarm optimizer (RSO) and nutcracker optimizer algorithm (NOA)) will be explored to automatically determine the ICNN model parameters, to enhance the model's feature learning performance even more.

Finally, although the presented fault diagnosis method has been successfully employed in bearing fault identification at constant operating speed, its diagnosis capability is still unknown for us at variable speed conditions. Consequently, based on the improvement of existing research and experimental conditions, by continuously improving our designed network model architecture and the entire implementation process of the proposed algorithms, our future efforts will be directed towards bearing fault identification in varying operating conditions.

5 Conclusions

This paper presents an improved wind turbine bearing fault diagnosis method predicated on POSGMD and an ICNN, which can strengthen fault

identification capability of wind turbine bearing under strong noise scenarios. Within the proposed method, with the help of relative entropy-based embedding dimension selection, POSGMD is initially presented to adaptively decompose the collected raw bearing vibration signals into several SGC. Meanwhile, signal reconstruction is conducted to obtain the reconstructed signal based on kurtosis-weighted criteria. Subsequently, the CWT of the reconstructed signal is computed to generate the corresponding time-frequency images. Finally, the acquired images are inputted into an ICNN for model training and automatic fault identification of rolling bearings. The efficacy of the presented approach is validated through two case studies. Empirical findings demonstrate that the suggested approach can attain superior identification precision amidst noisy conditions when juxtaposed with various exemplary fault diagnosis methodologies. The following encapsulates the primary innovations and contributions of this research:

1) By incorporating the relative entropy and kurtosis-weighted criteria into the original SGMD, this study proposes a POSGMD, which mitigates the over-decomposition or under-decomposition issues caused by inappropriate selection of the embedding dimension in SGMD.

2) By replacing the convolutional layers of conventional CNN with the designed convolutional block and residual block, an ICNN is proposed for robust feature learning and automatic fault identification, which can not only alleviate the vanishing issue during the training process of traditional CNN but also prevent the over-fitting problem in the network.

3) A novel bearing fault diagnosis method predicated on POSGMD and ICNN is proposed, which can enhance the fault identification precision under strong noise interference.

In future research, we aim to enhance the proposed method by incorporating multi-sensor information fusion technology. Single-sensor systems may miss critical fault information, while multi-sensor systems can capture complementary information to provide a more comprehensive view of equipment health. Specifically, we plan to develop an effective preprocessing strategy for multi-sensor signals, leveraging techniques such as principal component analysis (PCA) to reduce high-dimensional multi-channel data to three dimensions. These reduced-dimensional datasets will then be transformed into RGB image samples, facilitating input into advanced deep learning models. Furthermore, we intend to design lightweight and efficient deep network architectures to improve the accuracy of fault diagnosis while reducing computational costs, making the approach more suitable for real-time industrial applications. In addition, future work will test the enhanced method under real-world operating conditions with diverse and complex noise scenarios, ensuring robustness and generalizability. These advancements will contribute to developing a more powerful, reliable, and practical fault diagnosis system for wind turbine bearings and similar industrial equipment.

Acknowledgments

The authors want to gratitude to CWRU and SEU for supplying laboratory data.

References

[1] Peng H, Zhang H, Fan Y, et al. A review of research on wind turbine bearings' failure analysis and fault diagnosis. Lubricants, 2023, 11 (1): 14. DOI: 10.3390/lubricants11010014.

[2] Ye M, Yan X, Jiang D, et al. MIFDELN: A multi-sensor information fusion deep ensemble learning network for diagnosing bearing faults in noisy scenarios. Knowledge-Based Systems, 2024, 284: 111294. DOI: 10.1016/j.knosys.2023.111294.

[3] Ye M, Yan X, Jia M. Rolling bearing fault diagnosis based on VMD-MPE and PSO-SVM. Entropy, 2021, 23 (6): 762. DOI: 10.3390/e23060762.

[4] Guo J, Liu X, Li S, et al. Bearing intelligent fault diagnosis based on wavelet transform and convolutional neural network. Shock and Vibration, 2020: Article ID 6380486. DOI: 10.1155/2020/6380486.

[5] Zuo T, Zhang K, Zheng Q, et al. A hybrid attention-based multi-wavelet coefficient fusion method in RUL prognosis of rolling bearings. Reliability Engineering & System Safety, 2023, 237: 109337. DOI: 10.1016/j.ress.2023.109337.

[6] Wang J, Du G, Zhu Z, et al. Fault diagnosis of rotating machines based on the EMD manifold. Mechanical Systems and Signal Processing, 2020, 135: 106443. DOI: 10.1016/j.ymssp.2019.106443.

[7] Ge J, Niu T, Xu D, et al. A rolling bearing fault diagnosis method based on EEMD-WSST signal reconstruction and multi-scale entropy. Entropy, 2020, 22 (3): 290. DOI: 10.3390/e22030290.

[8] Wang T, Zhu T, Zhu L, et al. A fault diagnosis method

based on EEMD and statistical distance Analysis, Coatings, 2021, 11 (12): 1459. DOI: 10.3390/coatings11121459.

[9] Yang Y, Pan H, Ma L, et al. A roller bearing fault diagnosis method based on the improved ITD and RRVPMCD. Measurement, 2014, 55: 255-264. DOI: 10.1016/j.measurement.2014.05.016.

[10] Jin Z, He D, Wei Z. Intelligent fault diagnosis of train axle box bearing based on parameter optimization VMD and improved DBN. Engineering Applications of Artificial Intelligence, 2022, 110: 104713. DOI: 10.1016/j.engappai.2022.104713.

[11] Arrieta Paternina M R, Tripathy R K, Zamora-Mendez A, et al. Identification of electromechanical oscillatory modes based on variational mode decomposition. Electric Power Systems Research, 2019, 167: 71-85. DOI: 10.1016/j.epsr.2018.10.014.

[12] Cheng J, Yang Y, Li X, et al. An early fault diagnosis method of gear based on improved symplectic geometry mode decomposition. Measurement, 2020, 151: 107140. DOI: 10.1016/j.measurement.2019.107140.

[13] Chen W, Wang H, Li Z, et al. Gear fault diagnosis based on SGMD noise reduction and CNN. Journal of Advanced Mechanical Design, Systems, and Manufacturing, 2022, 16 (3): JAMDSM0031-JAMDSM0031.DOI: 10.1299/jamdsm.2022jamdsm0031

[14] Wang X, Zheng J, Pan H, et al. Maximum envelope-based autogram and symplectic geometry mode decomposition based gear fault diagnosis method. Measurement, 2021, 174: 108575. DOI; 10. 1016/j.measurement.2020.108575.

[15] Guo J, Si Z, Xiang J. Cycle kurtosis entropy guided symplectic geometry mode decomposition for detecting faults in rotating machinery. ISA transactions, 2023, 138: 546-561.DOI: 10.1016/j.isatra.2023.03.026.

[16] Liu Y, Cheng J, Yang Y, et al. The partial reconstruction symplectic geometry mode decomposition and its application in rolling bearing fault diagnosis. Sensors, 2023, 23: 7335.DOI: 10.3390/s23177335.

[17] Yan X, Liu Y, Jia M. A fault diagnosis approach for rolling bearing integrated SGMD, IMSDE and multiclass relevance vector machine. Sensors, 2020, 20: 4352.DOI: 10.3390/s20154352.

[18] Dong L, Chen Z, Hua R, et al. Research on diagnosis method of centrifugal pump rotor faults based on IPSO-VMD and RVM. Nuclear Engineering and Technology, 2023, 55: 827-838.DOI: 10.1016/j.net.2022.10.045.

[19] Wen L, Li X, Gao L. A transfer convolutional neural network for fault diagnosis based on ResNet-50. Neural Computing and Applications, 2020, 32: 6111-6124.DOI: 10.1007/s00521-019-04097-w.

[20] Tang S, Yuan S, Zhu Y. Deep learning-based intelligent fault diagnosis methods toward rotating machinery. IEEE Access, 2019, 8: 9335-9346. DOI: 10. 1109/ACCESS.2019.2963092.

[21] Wen L, Li X, Gao L, et al. A new convolutional neural network-based data-driven fault diagnosis method. IEEE Transactions on Industrial Electronics, 2017, 65: 5990-5998.DOI: 10.1109/TIE.2017.2774777.

[22] Hoang D T, Kang H J. A motor current signal-based bearing fault diagnosis using deep learning and information fusion. IEEE Transactions on Instrumentation and Measurement, 2020, 69: 3325-3333. DOI: 10.1109/TIM.2019.2933119..

[23] Cheng Y, Lin M, Wu J, et al. Intelligent fault diagnosis of rotating machinery based on continuous wavelet transform-local binary convolutional neural network. Knowledge-Based Systems, 2021, 216: 106796.DOI: /10.1016/j.knosys.2021.106796.

[24] Xu S, Yuan R, Lv Y, et al. A novel fault diagnosis approach of rolling bearing using intrinsic feature extraction and CBAM-enhanced InceptionNet. Measurement Science and Technology, 2023, 34 (10): 105111. DOI: 10.1088/1361-6501/ace19c.

[25] Hu H, Feng F, Zhu J, et al. Research on fault diagnosis method based on improved CNN. Shock and Vibration, 2022: Article ID 9312905. DOI: 10.1155/2022/9312905.

[26] He D, Liu C, Jin Z, et al. Fault diagnosis of flywheel bearing based on parameter optimization variational mode decomposition energy entropy and deep learning. Energy, 2022, 239: 122108. DOI: 10.1016/j.energy.2021.122108.

[27] Feng K, Ji J C, Zhang Y, et al. Digital twin-driven intelligent assessment of gear surface degradation. Mechanical Systems and Signal Processing, 2023, 186: 109896.DOI: 10.1016/j.ymssp.2022.109896.

[28] Ming Z, Tang B, Deng L, et al. Digital twin-assisted fault diagnosis framework for rolling bearings under imbalanced data. Applied Soft Computing, 2025, 168: 112528.DOI: 10.1016/j.asoc.2024.112528.

[29] Ni Q, Ji J C, Halkon B, et al. Physics-Informed Residual Network (PIResNet) for rolling element bearing fault diagnostics. Mechanical Systems and Signal Processing, 2023, 200: 110544.DOI: 10.1016/j.ymssp.2023.110544.

[30] Li S, Ji J, Feng K, et al. Composite neuro-fuzzy system-guided cross-modal zero-sample diagnostic framework using multi-source heterogeneous non-contact sensing data.IEEE Transactions on Fuzzy Systems, 2024, 33: 302-313.DOI: 10.1109/TFUZZ.2024.3470960.

[31] Li H, Li F, Jia R, et al. Research on the fault feature extraction of rolling bearings based on SGMD-CS and the AdaBoost framework. Energies, 2021, 14: 1555.DOI: /10.3390/en14061555.

[32] Pan H, Yang Y, Li X, et al. Symplectic geometry mode decomposition and its application to rotating machinery compound fault diagnosis. Mechanical Systems and Signal Processing, 2019, 114: 189-211. DOI: 10. 1016/j. ymssp. 2018.05.019.

[33] Liu S, Lu M, Liu G, et al. A novel distance metric:

generalized relative entropy. Entropy, 2017, 19: 269. DOI: 10.3390/e19060269.

[34] Lu Y, Xie R, Liang S Y. CEEMD-assisted kernel support vector machines for bearing diagnosis. The International Journal of Advanced Manufacturing Technology, 2020, 106: 3063-3070. DOI: 10.1007/s00170-019-04858-w.

[35] Chen X, Zhang B, Gao D. Bearing fault diagnosis base on multi-scale CNN and LSTM model. Journal of Intelligent Manufacturing, 2021, 32: 971-987. DOI: 10.1007/s10845-020-01600-2.

[36] Tang S, Zhu Y, Yuan S. An adaptive deep learning model towards fault diagnosis of hydraulic piston pump using pressure signal. Engineering Failure Analysis, 2022, 138: 106300. DOI;/10.1016/j.engfailanal.2022.106300.

[37] Zhang W, Peng G, Li C, et al. A new deep learning model for fault diagnosis with good anti-noise and domain adaptation ability on raw vibration signals. Sensors, 2017, 17: 425. DOI: 10.3390/s17020425.

[38] Jia Z, Liu J, Gao J, et al. Research on fault diagnosis method of induction motor bearing based on DACNN. 2024 Second International Conference on Cyber-Energy Systems and Intelligent Energy (ICCSIE). Piscataway: IEEE, 2024: 1-6. DOI: 10.1109/ICCSIE61360.2024.10698205.

[39] Xu M, Gao J, Zhang Z, et al. Bearing-fault diagnosis with signal-to-RGB image mapping and multichannel multiscale convolutional neural network. Entropy, 2022, 24(11): 1569. DOI: 10.3390/e24111569.